Pressure sensitivity of adiabatic shear banding in metals

E. Hanina, D. Rittel,[a),b)] and Z. Rosenberg[c)]
Faculty of Mechanical Engineering, Technion, 32000 Haifa, Israel

(Received 10 October 2006; accepted 5 December 2006; published online 10 January 2007)

Adiabatic shear banding (ASB) is a dynamic failure mode characterized by large plastic strains in a narrow localized band. ASB occurs at high strain rates ($\dot{\varepsilon} \geqslant 10^3\ s^{-1}$), under adiabatic conditions leading to a significant temperature rise inside the band [H. Tresca, Annales du Conservatoire des Arts et Métiers **4**, (1879); Y. L. Bai and B. Dodd, *Adiabatic Shear Localization-Occurrence, Theories, and Applications* (Pergamon, Oxford, 1992); M. A. Meyers, *Dynamic Behavior of Materials* (Wiley, New York, 1994).; and J. J. Lewandowski and L. M. Greer, Nat. Mater. **5**, 15 (2006)]. Large hydrostatic pressures are experienced in many dynamic applications involving ASB formation (e.g., ballistic penetration, impact, and machining). The relationship between hydrostatic pressure and ASB development remains an open question, although its importance has been often noted. This letter reports original experimental results indicating a linear relationship between the (normalized) dynamic deformation energy and the (normalized) hydrostatic pressure. © *2007 American Institute of Physics*. [DOI: 10.1063/1.2430923]

Adiabatic shear banding (subsequently referred to as ASB) failure is an instability which has drawn much attention from both the materials science community (microstructural aspects, e.g., Refs. 1 and 2 and the solid mechanics community (modeling, e.g., Ref. 3). ASB formation is traditionally explained by the competition between strain rate hardening and thermal softening until a critical instability strain is reached.[4] Recent experimental work[5] has suggested the dynamic deformation energy (integral of the stress-strain curve until failure) as an alternative initiation criterion. The energetic approach ties mechanical and microstructural issues through the fraction of mechanical energy that is elastically stored in the material (stored energy of cold work[5]), the rest being dissipated as heat.

The majority of studies to date investigate ASB formation under loading conditions that do not involve extra hydrostatic pressure, other than that encountered in uniaxial compression tests, e.g., Refs. 1 and 2, or in the absence of hydrostatic pressure, as in pure shear tests.[6–8] Yet, a substantial pressure component may develop in dynamic loading situations, such as ballistic impact and penetration, or machining of metals. In such cases, where ASB related failure is likely to occur, the influence of the hydrostatic pressure component on ASB formation has remained an essentially open question. Therefore, the present work was initiated to characterize the influence of hydrostatic pressure on ASB formation by means of a systematic experimental approach. Two materials were selected for this study: commercial AM50 (ASTM B94) magnesium aluminum alloy (as in Ref. 5) and a titanium alloy (Ti6AL4V), both supplied as extruded rods in the as-received condition. The experiments consisted of uniaxial compression of specimens that were encased in specially designed metallic sleeves. Figure 1 shows schematically the confining effect of the metallic sleeve on the cylindrical specimen. Cylindrical specimens were selected such that the ratio of the length over diameter was 1. The diameters were 8.0±0.01 mm for AM50 and 4.2±0.01 mm for Ti6Al4V. The specimen was encased in accurately machined sleeves made of as-received 4340 steel. For the AM50 alloy, the sleeves were 0.2, 0.4, and 0.6±0.005 mm thick, while for Ti6AL4V, we used 0.5 and 1±0.005 mm thick sleeves. The dynamic mechanical characteristics of the sleeve material were tested preliminarily for subsequent calculations of the confining pressure, and it was verified that this steel exhibits minimal strain hardening. The sleeve material and dimensions were optimized so that the confining pressure q was

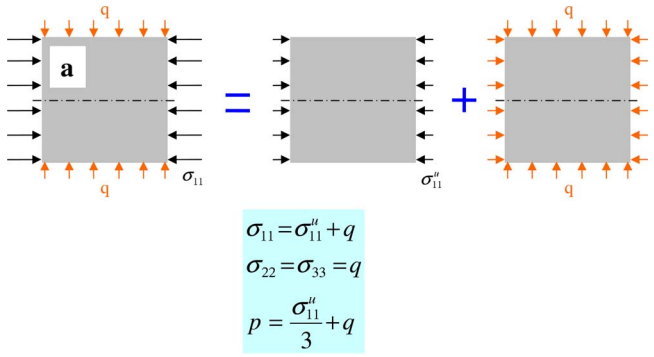

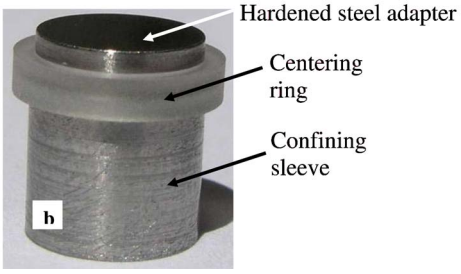

FIG. 1. (Color online) (a) Effect of confinement on the stress state of a cylindrical specimen. The symbols q, σ_{11}'', and p denote the confining pressure, unconfined uniaxial stress component, and hydrostatic pressure, respectively. During a test, σ_{11} is the measured stress component. (b) Confined specimen: The specimen is encased in a tightly fit steel sleeve. A hardened steel adapter applies the load to the specimen only. A polymeric ring is used to align the adapter with the specimen.

a)Authors to whom correspondence should be addressed.
b)Electronic mail: merittel@technion.ac.il
c)RAFAEL, POB 2250, Haifa, Israel.

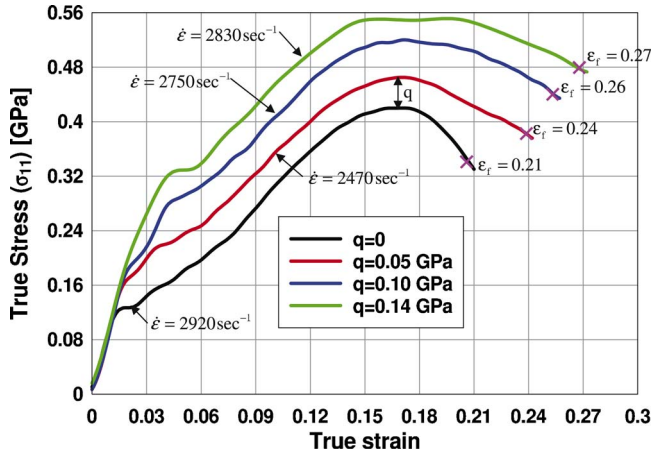

FIG. 2. (Color online) Typical dynamic stress-strain curves for AM50 specimens subjected to various confinement levels. As the confinement increases, the stress level translates upward. A larger confinement induces a larger failure strain (indicated by x) and a milder strain softening slope beyond the peak stress.

reasonably constant, starting from low strains (typically $\varepsilon \approx 0.05$). The specimen was loaded through a 2 mm thick rigid adapter made of hardened Maraging 250 steel (Fig. 1). The adapter diameter was carefully adjusted to that of the specimen to avoid loading of the sleeve. The adapter was aligned with the specimen by means of a polymeric centering ring. Dynamic tests were conducted on a 12.7 mm diameter, 250 Maraging steel Kolsky bar,[9] with the adapter always facing the incident bar. The uniaxial stress-strain curves were determined in a standard way after checking for dynamic equilibrium of the specimen. The confining pressure component q was directly measured, as shown in Figs. 1 and 2. It was also calculated using analytical approximations for a thin (or thick) elastic-plastic shell under internal pressure,[10] as well as finite element simulations. The failure strain ε_f was defined throughout this work as the strain at which the flow stress drops to 80% of its maximum value. This definition of the failure strain is arbitrary in the sense that the onset of failure cannot be precisely ascertained from a stress-strain curve. However, once the stress has dropped to 80% of its peak value, one can reasonably assume that ASB has fully developed in the specimen.[11] To allow for comparison between the two materials tested, the failure strain, hydrostatic pressure, and dynamic mechanical energy were all normalized. The reference state is that of the uniaxial, unconfined compression test. The normalized pressure is defined as $\tilde{P} = p/\sigma^{\mu}_{11\,\max}$, where p is the hydrostatic pressure and $\sigma^{\mu}_{11\,\max}$ is the peak stress experienced by the unconfined specimen. Consequently, $\tilde{P} = 1/3$ corresponds to unconfined uniaxial compression.

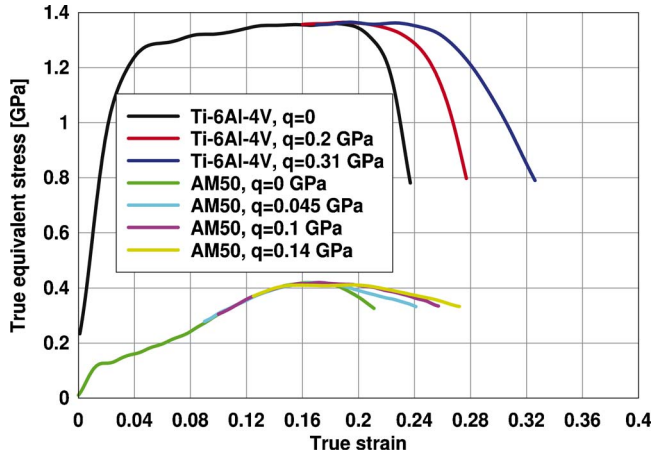

FIG. 3. (Color online) Typical dynamic equivalent stress-strain curves for AM50 and Ti6Al4V specimens. The confining hydrostatic pressure q has been subtracted to emphasize the effect of confinement on the flow curve of these alloys.

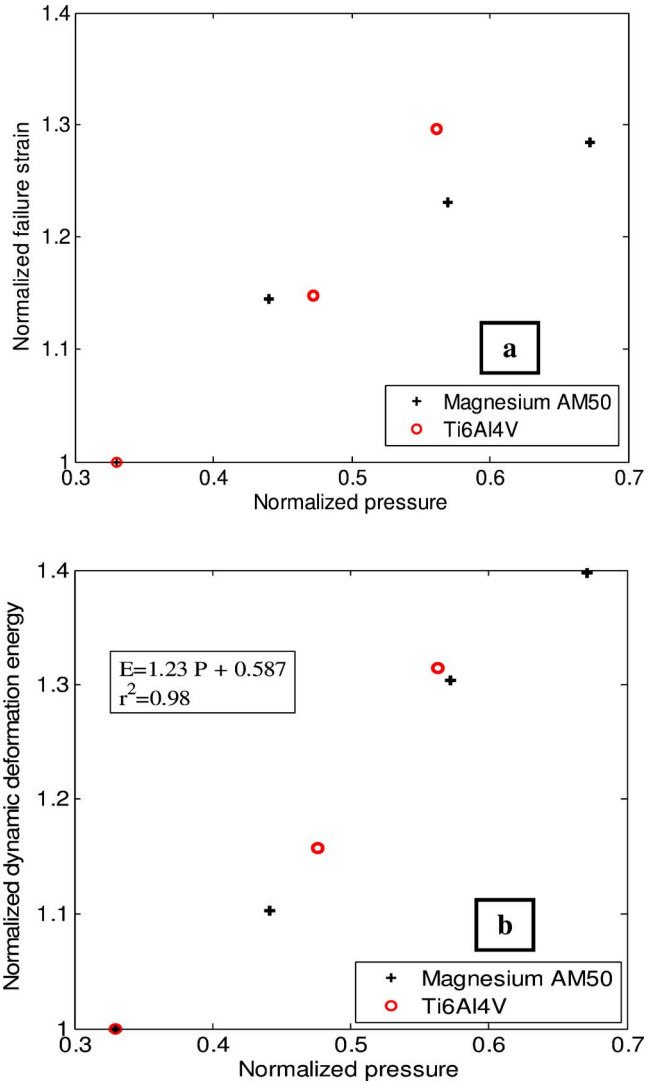

FIG. 4. (Color online) (a) Plot of the normalized failure strain vs normalized hydrostatic pressure. The reference state is that of a uniaxial, unconfined compression test. The pressure is normalized vs the peak stress experienced by this specimen. Consequently, a uniaxial unconfined specimen is represented by the coordinates (1/3, 1). (b) Plot of the normalized dynamic mechanical energy vs normalized hydrostatic pressure. The reference state is, as before, that of a uniaxial, unconfined compression test. Note that the response of the two investigated alloys lies on a single straight line.

Figure 2 shows a typical dynamic stress-strain curve for AM50 under various regimes of confinement. All the specimens failed by ASB formation, with the failure strain being denoted by x. As expected, higher hydrostatic pressures cause an increasing offset of q in the flow stress of the material, allowing for its determination. The results obtained for AM50 and Ti6Al4V alloys are summarized in Fig. 3, after subtraction of the confining stress q. Figure 3 shows that Ti6Al4V exhibits a small dynamic strain hardening capacity, as opposed to AM50. Figures 2 and 3 show two distinct

effects of the confinement. First, the failure strain (at 80% of peak stress value) increases with the pressure, similar to results reported for quasistatic tests.[12] In addition, the slope of the falling stress past its peak value is increasingly milder as the pressure is increased. Therefore, the hydrostatic pressure not only increases the failure strain but it also confers a less catastrophic character to the final failure process. The normalized failure strain is plotted as a function of the normalized hydrostatic pressure in Fig. 4(a), for the two investigated materials. This figure shows that each material responds differently to the application of hydrostatic pressure. The results are replotted in Fig. 4(b), in which the dynamic deformation energy[5] is plotted this time, instead of the failure strain. The normalized dynamic energy is calculated by integrating the stress-strain curve up to the failure strain after subtraction of the confining hydrostatic pressure q, as shown in Fig. 3. This reflects the well-known fact that metal plasticity is not influenced by hydrostatic pressure. The dynamic deformation energy is normalized by that of a nonconfined uniaxial compression test. Figure 4(b) reveals that the adiabatic shear banding response of the two alloys is linearly related to the normalized hydrostatic pressure.

The novelty of this work resides in the systematic investigation of hydrostatic pressure effects that were not previously addressed in the literature. The strength of the dynamic deformation energy concept is that it reconciles seemingly different results [Fig. 4(a)] into a single curve [Fig. 4(b)]. It is interesting to note that ASB formation, as a plastic instability phenomenon, is expected to be insensitive to hydrostatic pressure. Yet, the present results indicate a definite sensitivity to pressure which can therefore only be attributed to those pressure-sensitive internal damage micromechanisms operating in the shear band (e.g., void nucleation and growth, and dynamic recrystallization[1,2]) once it has formed. This comes along with the decreasing slope of the stress-strain curve beyond the peak stress, indicating a more controlled type of failure mechanism inside the shear band, in other words a reduced damage development rate with increasing pressure. The generality of the linear relationship shown in Fig. 4(b) should be further established by performing similar tests on other metals with extended confinement pressures.[13] Nevertheless, the present results indicate a clear trend in the correlation between ASB formation and hydrostatic pressure in metallic materials.

To summarize, until now, the influence of hydrostatic pressure on ASB formation has been largely unexplored. This work shows, first of all, that the failure strain for adiabatic shear banding increases with hydrostatic pressure. The results also suggest that hydrostatic pressure delays those pressure-sensitive damage phenomena that develop in the shear band, leading to final failure. Moreover, this work shows a linear relationship between the normalized dynamic deformation energy[5] and pressure for all three alloys [Fig. 4(b)]. These results can be used to introduce an alternative failure criterion into numerical simulations of high rate impact in which large hydrostatic pressures develop along with ASB failure.

The support of the Israel Science Foundation (Grant No. 2006046) is gratefully acknowledged.

[1] Y. L. Bai and B. Dodd, *Adiabatic Shear Localization-Occurrence, Theories and Applications* (Pergamon, Oxford, 1992).
[2] M. A. Meyers, *Dynamic Behavior of Materials* (Wiley, New York, 1994).
[3] T. W. Wright, *Physics and Mathematics of Adiabatic Shear Bands* (Cambridge University Press, Cambridge, 2002).
[4] C. Zener and J. H. Hollomon, J. Appl. Phys. **15**, 22 (1944).
[5] D. Rittel, Z. G. Wang, and M. Merzer, Phys. Rev. Lett. **96**, 075502 (2006).
[6] D. R. Chichilli and K. T. Ramesh, J. Appl. Mech. **66**, 10 (1999).
[7] D. R. Chichilli, K. T. Ramesh, and K. J. Hemker, J. Mech. Phys. Solids **52**, 1889 (2004).
[8] A. Marchand and J. Duffy, J. Mech. Phys. Solids **36**, 251 (1988).
[9] H. Kolsky, Proc. R. Soc. London, Ser. B **62**, 676 (1949).
[10] C. Y. Warren and G. B. Richard, *Roark's Formulas for Stress and Strain*, 7th ed. (McGraw-Hill, New York, 2002).
[11] We performed real-time temperature measurements of the gauge section during high rate impact experiments of the AM50 and Ti6AL4V alloys. These measurements clearly show a very mild temperature rise until the peak stress level, followed by a very significant rise in the falling section of the stress-strain curve. These measurements support the present identification of a failure strain as the strain at which an adiabatic shear band has fully developed, in which the large concentrated strain leads to a significant temperature rise.
[12] K. Osakada, A. Watadani, and H. Sekiguchi, Bull. JSME **20**, 1557 (1977).
[13] A key component of the experimental specimen is the metal sleeve. The latter must exhibit little strain hardening and high strength to apply constant high levels of confinement. However, low hardening materials tend to exhibit plastic localization (e.g., necking) at relatively small strains, thus limiting the maximum strain that can be applied to the confined specimen. AM50 and Ti6Al4V alloys are well suited for these experiments due to their relatively low failure strains.